

**Title: Genesis of Active Sand-filled Polygons in Lower and Central Beacon
Valley, Antarctica**

James G. Bockheim^{*}

Mark D. Kurz^{**}

S. Adam Soule^{**}

Andrea Burke^{**}

^{*}Department of Soil Science, University of Wisconsin, 1525 Observatory Drive, Madison, WI 53706-1299, U.S.A. Corresponding author: bockheim@wisc.edu

^{**} Woods Hole Oceanographic Institution, Woods Hole, MA, 02543 U.S.A.

Corresponding Author: J.G. Bockheim; email: Bockheim@wisc.edu; Tel. 1-608-263-5903; fax 1-608-265-2535.

ABSTRACT

Nonsorted polygons with sand-filled wedges were investigated in lower and central Beacon Valley, Antarctica (77.82°S , 160.67°E) using field observations coupled with a 2-m resolution Digital Elevation Model and a high-resolution aerial photograph. A gasoline-powered concrete breaker was employed to expose the sediments of four representative polygon centers and six wedges from geomorphic surfaces containing tills of two different ages. The excavated polygons ranged from 9 to 16 m in diameter (average = 12 m); the sand-filled wedges ranged from 0.2 m to 2.5 m in width (average = 0.9 m). The top of ice-bonded permafrost ranged from 12 to 62 cm in depth (average = 33 cm) in the polygon centers and from 64 to >90 cm (average = >75 cm) in wedges. One active thermal contraction fissure generally was apparent at the surface, but excavations revealed numerous inactive fissures. The wedges contain sand laminations averaging 3 mm in width when viewed in cross section. Although most of the polygons were of the sand-wedge type, some contained ice veins up to 1 cm in width and could be classed as composite wedges. Three stages of polygon development were observed, including strongly developed polygons on Taylor II surfaces (ca. 117 ka), moderately developed polygons on Taylor III surfaces (ca. 200 ka), and poorly developed polygons on Taylor IVa and older (ca. >1.1 Ma) surfaces. This retrogressive development may be due to sublimation of ice-bonded bonded permafrost following thermal cracking. With the drop in ice content, the thermal coefficient of expansion is lowered, which causes a reduction in tensile stresses.

Keywords: sand-wedge polygons, patterned ground, non-sorted polygons, thermal contraction fissures, McMurdo Dry Valleys, permafrost

INTRODUCTION

Since the early work of T.L. Péwé (1959) and R.F. Black (Berg and Black, 1966; Black, 1973) in the McMurdo Dry Valleys of Antarctica, there have been few investigations of the mechanisms of active sand-wedge formation. Péwé (1959) studied the approximate size and composition of thermal contraction fissures in Antarctica, and Berg and Black (1966) and Black (1973) measured wedge growth rates from permanent plots and attempted to use this information to date landforms. Ugolini et al. (1973) proposed two stages of nonsorted polygon formation in Beacon Valley that included well-developed polygons and poorly expressed polygons. Marchant et al. (2002) depicted the key stages in formation of high-centered polygons over buried glacier ice in upper Beacon Valley ($S77^{\circ}51.039'$, $E160^{\circ}35.576'$). Sletten et al. (2003) described the initiation and maturation of patterned ground, largely from measurements of 60-cm long rods hammered vertically into the ground on opposite sides of contraction cracks in lower Beacon Valley. Levy et al. (2006) focused on the geometry of patterned ground on rock glaciers and sublimation till in upper Beacon Valley.

There have been numerous studies of inactive sand-wedge polygons containing permafrost, primarily in the Canadian Arctic (Murton, 1996; Murton and French, 1993; Murton and Bateman, 2007). In addition, sand-wedge relicts have been observed in many areas where permafrost formerly existed and have been used in paleo-environmental reconstruction, including northern Alaska (Carter, 1983), eastern New Jersey, USA (French et al., 2003), the Hexi Corridor, China (Wang et al., 2003), Flanders, Belgium (Ghysels and Heyse, 2006), and north-central Hungary (Kovács et al., 2007).

The objectives of this study were to: (1) describe and characterize sand-filled wedges and polygons, (2) interpret these features, and (3) propose a descriptive model for the formation of

sand-filled polygons in lower and central Beacon Valley from detailed analysis of a digital elevation model (DEM) with a 2-m resolution and other information.

STUDY AREA

Located in the Quartermain Mountains, Beacon Valley is 17 km long and 3 km wide (Fig. 1). The valley trends upward northeast to southwest, with the valley floor rising from 930 m near the Taylor Glacier to over 1,600 m in the uppermost part of the valley. The bedrock is comprised of sandstones from the Devonian-to-Jurassic Beacon Supergroup that have been intruded by sills and dikes of Ferrar dolerite during the Jurassic (Barrett, 1981). Reconnaissance glacial geomorphology maps of Beacon Valley were prepared by Linkletter et al. (1973), Sugden et al. (1995), and Bockheim (2007). Based on differences in moraine morphology, surface boulder weathering, and soil development, at least five drift sheets have been distinguished in Beacon Valley and the nearby Arena Valley. These include Taylor II, Taylor III, Taylor IVa, Taylor IVb, and Granite till, which are believed to be 117 ka, 200 ka, 1.0-2.2 Ma, >2.2 to <7.4 Ma, and 8 Ma in age, respectively, based on cosmogenic nuclides, volcanic-ash dating, and stratigraphic and geometric relations of drifts (Brook et al., 1993; Marchant et al., 1993; Sugden et al., 1995). The drift sheets and recessional moraines along the valley floor are thin, ranging from one to several meters in thickness.

Soils of Beacon Valley generally contain ice-bonded permafrost within 100 cm of the surface and, compared to the nearby Arena Valley, have higher moisture contents and lower levels of salts (Bockheim, 2007). The following properties increase with age on glacial drifts of Beacon Valley: weathering stage, morphogenetic salt stage, electrical conductivity of the horizon of maximum salt accumulation, and depth of staining.

From temperature measurements in a borehole at a depth of 19.6 m, the mean annual air temperature of Beacon Valley is approximately -23°C (Sletten, personal communication). The mean monthly air temperature of the coldest months, June through August, is approximately -35°C and the mean monthly temperature for the warmest months, December through February, is about -10°C. There are very few days when the air temperature rises above 0°C. The mean annual precipitation is ca. 100 mm/yr (water equivalent). Frequent snowfalls followed by strong winds may selectively contribute snowfall to polygon wedges. However, our observations suggest that little of this snow melts; rather, the snow is lost in late summer due to sublimation.

The region contains continuous permafrost. However, the upper part of the permafrost often is “dry” in that it contains very low concentrations of ice (<5% by weight) and is, therefore, loose. Ice-bonded permafrost contains about 10 to 15% ice. The active-layer depth, which must be determined from closely spaced thermisters, ranges from 20 to 30 cm in thickness.

METHODS

A manual examination was conducted of polygon dimensions, including size and shape of polygons and width and depth of wedges from the Beacon Valley Digital Elevation Model (DEM), which has a 2-m resolution (U.S. Geological Survey and Ohio State University), a scanned, high-resolution, high-elevation, oblique color air photograph (USGS), and the authors' personal photographs taken during helicopter flights. Our observations of patterned ground were made on drift sheets along an approximate 400-m wide longitudinal profile down the center of the valley where valley sidewalls had minimal influence, with an emphasis on lower and central Beacon Valley. Although we avoided excavating on moraine crests, we recognized the

termination of Taylor II, III, and IVa drifts as being 2.1, 4.9, and 9.8 km southwest of the Taylor Glacier, respectively (Fig. 1).

Recognized polygons shapes identified previously in Antarctica include rectangular, pentagonal, hexagonal, heptagonal, and octagonal, and recognized polygon forms include high-centered and flat-centered (Berg and Black, 1966; Black, 1973). Five representative polygons were selected on Taylor II and Taylor III drifts. There was insufficient time to excavate on older drifts. Selected polygons were of average form and size on a particular drift and were located away from boulder-belt moraines and valley walls. Because they were most common on Taylor II and III drifts, all of the polygons excavated were of the high-center type. A gasoline-powered concrete breaker (Wacker Incorporated ©) was employed to excavate within the polygon centers and the wedges.

Cross-sectional diagrams were prepared for four of the six sand-filled wedges using the technique described by Bockheim and Tarnocai (1998). The stratigraphy along a cross-sectional profile was examined qualitatively, including field textures, nature of the fabric, distribution, form and relative amount of ice, and shape and degree of frosting of infilled sand grains.

Although a primary aim of this study was to characterize sand-filled wedges in lower and central Beacon Valley, soils were important in preparing our descriptive model of polygon formation. Soil profiles were described, weathering stages and morphogenetic salt stages were determined (Bockheim, 2007), and the soils were classified according to *Soil Taxonomy* (Soil Survey Staff, 2006). Color development equivalence (CDE) was determined using the system of Buntley and Westin (1965). In addition to data collected during the study, we utilized unpublished data from the 1969 notes of J. Bockheim on Taylor IVa surfaces in central Beacon Valley. A descriptive model was developed from the aforementioned data.

RESULTS

Polygon morphometrics

The excavated polygons ranged from 9 to 16 m in diameter (average = 12 m), 80 m² to 240 m² in area (average = 159 m²), and the sand-filled wedges ranged from 0.2 m to 2.5 m in width (average = 0.9 m) (Table 1). We were able to excavate in wedges to depths ranging from 50 to 130 cm (average = 86 cm). Because the depth to ice-bonded permafrost averaged 29 cm, we excavated an average of 57 cm into ice-bonded permafrost.

From analysis of the DEM, polygons on Taylor II drift were commonly high-centered, pentagonal to heptagonal in shape, and had an area of about 100 m² (Figs. 2A and 3A). The troughs averaged 0.5 m in width and 1 m in depth (Table 1). Polygons on Taylor III drift were often high-centered and had a pentagonal or hexagonal shape (Figs. 2B and 3B). The polygons were comparable in size to those on Taylor II drift. However, the wedges were wider, averaging 2 m, and less deep (average = 1 m). Polygons on Taylor IVa drift were more diffuse than those on younger drifts. Due to wind-blown snow accumulating in the wedges, only two or three sides of the polygons often were visible. The wedges were very broad often reaching 6 m but averaging 3 m in width. We observed very few rims on either side of the polygon wedges.

Stratigraphy of polygon centers and wedges

In polygon centers, the top of ice-bonded permafrost or buried ice ranged from 12 to 72 cm in depth (average = 33 cm). Two of the polygon centers were underlain by relatively pure, gray buried ice. The unfrozen portions of wedges had a steep “V” shape on Taylor II surfaces (Figs.

4A, 5A, 5B) and a broadened “V” shape on Taylor III surfaces (Fig. 5C). The maximum depth to the top of ice-bonded permafrost in wedges ranged from 64 to more than 90 cm (Table 1).

Following the terminology of the *Soil Survey Manual* (Soil Survey Divisional Staff, 1993), polygon centers were comprised of cobbly (75 to 250 cm) or gravelly (2 mm to 75 cm) sand, and the wedges were cobbly or gravelly sands in the upper 20 to 40 cm (Fig. 4A), but with pure sand below. Although active single fissures were visible in wedges when viewed in plan section, inactive cracks filled with sand were seen below the surface (Fig. 4C). The typical cross-sectional profile of a wedge contained a series of sand laminations arranged in a V-shaped network. Clasts having fallen into the fissures appeared to have interrupted the flow of sand, creating columns of sandy material (Fig. 4D). Multiple flow lines of infilling sand were viewed in sections across the wedges, especially in older sand-filled wedges (Fig. 4C). When viewed in long section, these features resembled bundles of parallel sand laminations (Fig. 4E). Individual laminations averaged 3 mm in width. Mineral grains in the fissures, particularly quartz, were well rounded and frosted. We did not observe upturned sediments adjacent to the wedge when it was viewed in cross-section.

Ice was occasionally found in the fissures, generally as veins up to 1 cm in width but also as lenses up to 5 mm in thickness (Fig. 4F). The ice-bonded permafrost surrounding the wedges was of a concrete type with most of the pores filled with ice.

Soil development

The soils show a general progression in development from Taylor II to Taylor IVa surfaces within polygon centers and within polygon wedges (Table 3). Within polygon centers and the wedges, the following properties commonly increased with an increase in approximate age of the drift:

depth to the base of oxidation, maximum color-development equivalence (CDE), depth to the surface of ice-bonded permafrost, and weathering stage. Soils in polygon centers were more strongly developed than those in polygon fissures on Taylor II and III moraines. However, on Taylor IVa drift, soils in polygon centers were comparable in development to those in wedges.

DISCUSSION

Interpretation of nonsorted polygons

The polygons examined in this study are primarily sand-wedge polygons. A few of the polygons contain lenses and veins of ice that comprise less than 2% of the total volume of the wedge; these may be classed as composite polygons. The polygons appear to have formed from sand falling into thermal contraction fissures and resemble those reported by Péwé (1959) and Berg and Black (1966).

Descriptive model of sand-wedge formation

At least four descriptive models for sand-wedge formation have been developed for Beacon Valley alone (Table 4). The model of Ugolini et al. (1973) is largely a retrogressive model in which high-center polygons continue to develop for a period of time and then undergo a flattening and the wedges become wider with additional time. The models of Marchant et al. (2002) and Levy et al. (2006) deal specifically with the key stages in the formation of high-centered polygons over buried glacier ice in upper Beacon Valley and bear only peripherally on our study. They also are retrogressive models because they evoke a negative feedback through which secondary ice formation is proposed to terminate further thermal contraction. As the troughs enlarge, they collect wind-blown snow from the polar plateau. This snow retards sublimation of buried ice by

reducing the vapor-pressure gradient. Because of their insulating effect, snow and slumped material in deep troughs may terminate further contractions. Marchant et al. (2002) used this model to explain the persistence of buried ice for periods of up to 8 million yr.

In contrast to the previously mentioned models, the model of Sletten et al. (2003) is progressive and is based on measurements of displaced rods driven into the permafrost 40 years earlier by Berg and Black (1963). They proposed three stages in sand-wedge development: an initial phase ($10\text{-}10^3$ years), a developmental phase ($10^3\text{-}10^4$ years), and a mature phase ($10^4\text{-}10^6$ years). During development, sand wedges become progressively wider with time, causing the formation of “shoulders” (rims) adjacent to the fissures and aggradation of polygon centers due to expansion and deformation.

Based on our field observations and image analyses, we propose an additional model for sand-wedge formation in lower and central Beacon Valley (Fig. 6). During the initial stages of sand-wedge formation, fissures propagate upward through the overlying drift when the tensile stresses induced by the cooling of the ground and subsurface reach the tensile strength of the underlying ice-bonded permafrost. These fissures typically are 0.5 to 2 cm in width and in plan view are reflected in the summer by “dimples” of flowing sand (Fig. 7). Fracturing results in a polygonal network of approximately 100 m^2 in plan view.

Over time fissures become filled with sand during sand-wedge formation creating V-shaped wedges. The sand originates partially from collapse of polygon sides and partially from wind deposition. With repeated cracking, loose sand moves downward into the contraction fissures, leaving a coarse-grained gravel and cobble lag at the base of the wedge. Lowering of the surface of the ice-bonded permafrost table in the sand-wedge is due primarily to the loss of matrix ice due to sublimation. Ice-bonded permafrost in Beacon Valley often contains only 10 to 15% moisture

by weight (Black, 1973). In contrast, sand in the fissures has between 2 and 4% moisture. The pores within the sand-filled fissure have a lower thermal capacity than the ice in ice-bonded permafrost (Burn, 2004). The drop in ice content may lower the coefficient of linear expansion in accounting for the lowering of tensile stresses. Eventually, the polygons centers become smaller and have less relief as the wedges spread and the fissures eventually become inactive. On Taylor IVa drift in central Beacon Valley, the lack of contraction fissures suggests that many of the polygons are no longer active.

A key difference in the descriptive models of sand-wedge development pertains to the mechanism of displacement of materials as the wedge grows laterally. Sletten et al. (2003) proposed a convection-like system similar to what occurs with ice-wedge formation in the arctic (Mackay, 1986), whereby there is an upward “bulging,” i.e., aggradation of the polygon surface. They suggested that eventually the entire polygon becomes underlain by reworked materials from sand-wedge formation, and they proposed that the polygon materials could be reworked in as little as 10^4 years. In contrast, we found no evidence for convection flow or deformation of polygon edges and centers in lower and central Beacon Valley. Moreover, Sletten et al. (2003) reported rims of compressed sand along the edges of wedges accompanied by upwarping of sediments adjacent to the wedge when viewed in cross section. However, we did not observe these features.

According to our model, once fissures form, sand and gravel from the side of the polygon fall into the fissure (Fig. 6). The trough widens with time creating a characteristic V shape. There is some displacement of material alongside the fissure; however, we saw minimal evidence of “shoulders” (rims) in lower and central Beacon Valley. Because the lag deposits in the trough are sufficiently permeable to permit enhanced conductive cooling during the winter months, they tend

to favor repeated thermal contraction sites. Fissures may become blocked by trapped gravel and cobbles that create sand columns (Fig. 4D). The fissures tend to migrate laterally across the wedge over time when view in plan section. Once the wedges become deep enough, windblown sand may become a primary source of material to the wedges.

The buildup of material in the wedge causes a localized depression in the underlying ice-bonded permafrost table. Whereas the depth to ice-bonded permafrost ranges from 12 to 62 cm (average = 33 cm) in the polygon center, it ranges from 64 to >90 cm (average = >75 cm) in the wedge. With our model, there is no need to invoke mechanical convection within the frozen polygon center and aggradation, as was proposed by Sletten et al. (2003). This is supported by our soils examinations. Soils within polygon centers have a comparable development to those on moraine crests that lack high-centered polygons. In addition, soils in both polygon centers and polygon fissures show progressive development with time (Ugolini et al., 1973; Bockheim, 2007), which argues against extensive convective cycling in polygon centers and continued wedge growth for periods up to 10^6 years.

Polygons in Mullins Valley in upper Beacon Valley are oriented down-valley because of rapid flow of underlying rock glaciers (Levy et al., 2006). The same is true of polygons on Taylor IV drift in central Beacon Valley (Figs. 1, 3C). However, this distortion is not apparent in patterned ground on Taylor II and III drifts, either because they are not underlain by rock glaciers or because the rock glaciers are no longer active. Although Péwé (1959) suggested that sand wedges may theoretically extend to depths of 5 m, our preliminary excavations yielded fissure depths of 0.6 m to approximately 1.5 m (Table 1).

Retrogression of patterned ground development

Field observations and examination of the Beacon Valley DEM and color air photographs support an eventual degradation of high-centered polygons. The number of polygon sides visible diminishes with time. Whereas high-centered polygons were common on Taylor II and III surfaces, flat-centered polygons were prevalent on Taylor IVa surfaces. With time, the width of the polygon wedges increases and the depth of the wedges decreases.

In lower Beacon Valley well-developed polygons occur primarily on Taylor II surfaces that are 117 ka in age. An examination of Black's original 14 patterned ground monitoring sites revealed that all but the two at Nussbaum Riegel in Taylor Valley occur on surfaces \leq 117 ka in age. According to our model, poorly expressed polygons exist on older surfaces except where there is a pronounced local moisture supply. At Nussbaum Riegel moisture is supplied by streams from the Kukri Hills and freshwater ponds. Eventually the polygons become more subdued and the fissures broaden to widths of 6 m or more (Fig. 3C).

The presence of diffuse polygons is not unique to central Beacon Valley. They are also found on Taylor III (208-335 ka), Taylor IV (ca. 1.1- $<$ 3.5 Ma), and Alpine III ($<$ 3.5 Ma) in Taylor Valley and on Miocene-aged surfaces in the Asgard Range (Bockheim, personal observations). In addition, many Pliocene and older surfaces in the McMurdo Dry Valleys lack patterned ground but the soils contain sand-wedge casts that attest to the former presence of ice-bonded permafrost and patterned ground (Bockheim, 2007). It is interesting that Berg and Black (1963, p. 125) suggested: "Growth rates of sand wedges theoretically will diminish with time as loose sand is added to the ground, leaving small cores of ice-cemented material in the centers of polygons too small to crack under the seasonal temperature changes."

Finally, we express concern over the use of sand-wedge growth to date landforms. Berg and Black (1966) recognized several sources of error in measurement of wedge growth rates,

including limitations of the measuring devices, the quality of measuring points (e.g., tilting of rods), stake movement, and personnel factors. In addition to these, we question growth rates estimated from rods penetrating only 2 to 12 cm into ice-bonded permafrost. Contraction sites 6 and 7 in Beacon Valley yielded dates of 3 to 5 ka as estimated from patterned ground growth rates (Berg and Black, 1966). In contrast, cosmogenic dating of equivalent moraines traced to the nearby Arena Valley yielded an age of 117 ka for Taylor II drift (Brook et al., 1993).

CONCLUSIONS

Sand-wedge polygons in Beacon Valley reach a maximum state of development achieved over ca. 117,000 yr and then regress with further time. Well-developed, nonsorted high-center polygons occur on surfaces up to 117,000 yr. However, on older surfaces the polygons become more subdued and the wedges become broader, attaining widths of 6 m. Our findings of sand-wedge development support those of Berg and Black (1966) in that a thaw bulb in ice-bonded permafrost develops in the sand wedge. Although we did not observe rims or other evidence of deformation near the margin or center of polygons, these features occur in Victoria Valley and other areas of the McMurdo Sound region (Berg and Black, 1966).

Excavations in polygon centers and sand wedges yield pertinent information regarding the stratigraphy, fabric, and distribution of ice in patterned ground of Beacon Valley. Sand wedges have a characteristic V shape but fissures are not limited to a single location. Instead, these fissures appear to migrate as they become plugged with coarse fragments. In lateral view, infilling fissures resemble rivulets of flowing sand. There is some segregated ice in sand wedges, primarily as ice veins but also as ice lenses. In contrast the surrounding ice-cemented permafrost

is of a concrete type. The segregated ice in sand wedges probably originates from unusual warming events that melt snow accumulated in polygon wedges.

ACKNOWLEDGMENTS

This research was supported by NSF grant OPP06336629 to MK. The authors appreciate the support of Raytheon Polar Services and Petroleum Helicopters, Inc. K.M. Hinkel and J. Munroe kindly read an earlier draft of this manuscript. We are grateful to G. Ghysels, I. Heyse, A. Lewkowicz, and “the wedgster” for highly constructive reviews of this paper.

REFERENCES

- Barrett PJ. 1981: History of the Ross Sea region during the deposition of the Beacon Supergroup 400-180 million years ago. *Journal of the Royal Society of New Zealand* **11**: 447-458.
- Berg, TE, Black RF. 1966. Preliminary measurements of growth of nonsorted polygons, Victoria Land, Antarctica. *Antarctic Research Series* **8**: 61-108. American Geophysical Union, Washington, D.C.
- Black RF. 1973. Growth of patterned ground in Victoria Land, Antarctica. In: *Permafrost: North American Contribution to the Second International Conference*, pp. 193-203, National Academy of Sciences, Washington, D.C.
- Bockheim JG. 1990. Soil development rates in the Transantarctic Mountains. *Geoderma* **47**: 59 77.
- Bockheim JG. 2007. Soil processes and development rates in the Quartermain Mountains, upper Taylor Glacier region, Antarctica. *Geografiska Annaler* **89A**(3): 153-165.
- Bockheim JG, Tarnocai C. 1998. Recognition of cryoturbation for classifying permafrost-affected soils. *Geoderma* **81**: 281-293.
- Brook EJ, Kurz MD, Ackert R Jr., Denton GH, Brown ET, Raisbeck GM, Yiou E. 1993. Chronology of Taylor Glacier advances in Arena Valley, Antarctica, using *in-situ* cosmogenic ^{3}He and ^{10}Be . *Quaternary Research* **39**: 11-23.
- Burn, C.R. 2004. The thermal regime of cryosols. In: *Cryosols; Permafrost-Affected Soils*. Ed. by JM Kimble, Springer, Berlin, pp. 391-413.
- Buntley GJ, Westin FC. 1965. A comparative study of developmental color in a chestnut chernozem-brunizem soil climosequence. *Soil Science Society of America Proceedings* **29**:

- 579-582.
- Campbell IB and Claridge GGC. 1975. Morphology and age relationships of Antarctic soils. In: Suggate RP, Creswell MM (eds.) *Quaternary studies*. The Royal Society of New Zealand, Wellington, pp. 83-88.
- Carter LD. 1983. Fossil sand wedges on the Alaskan Coastal Plain and their paleoenvironmental significance. In: *Permafrost, Fourth International Conference Proceedings*, pp. 109-114. National Academy of Sciences Press, Washington, D.C.
- French HM, Demitroff M, Forman SL. 2003. Evidence for late-Pleistocene permafrost in the New Jersey Pine Barrens (latitude 39°N), eastern USA. *Permafrost and Periglacial Processes* **14**: 259-274.
- Ghysels G, Heyse I. 2006. Composite-wedge pseudomorphs in Flanders, Belgium. *Permafrost and Periglacial Processes* **17**: 145-161. DOI: 10.1002/ppp.552
- Kovács J, Fábián SA, Schweitzer F, Varga G. 2007. A relict sand-wedge polygon site in north central Hungary. *Permafrost and Periglacial Processes* **18**: 379-38. DOI: 10.1002/ppp.600.
- Levy JS, Marchant DR, Head JW III. 2006. Distribution and origin of patterned ground on Mullins Valley debris-covered glacier, Antarctica: the roles of ice flow and sublimation. *Antarctic Science* **18**: 385-397. DOI: 10.1017/S0954102006000435
- Linkletter GO, Bockheim J, Ugolini FC. 1973. Soils and glacial deposits in the Beacon Valley, southern Victoria Land, Antarctica. *New Zealand Journal of Geology and Geophysics* **16**: 90-108.
- Mackay JR. 1986. The first 7 years (1978-1985) of ice wedge growth, Illisarvik experimental drained lake site, western Arctic coast. *Canadian Journal of Earth Sciences* **23**: 1782-1795.
- Marchant DR, Denton GH, Swisher CC III. 1993: Miocene-Pliocene-Pleistocene glacial

- history of Arena Valley, Quartermain Mountains, Antarctica. *Geografiska Annaler* **75A**: 269-302.
- Marchant DR, Lewis AR, Phillips WM, Moore EJ, Souchez RA, Denton GH, Sugden DE, Potter N Jr, Landis GP. 2002: Formation of patterned ground and sublimation till over Miocene glacier ice in Beacon Valley, southern Victoria Land, Antarctica. *Geological Society of America Bulletin* **114**: 718-730.
- Murton JB. 1996. Morphology and paleoenvironmental significance of Quaternary sand veins, sand wedges, and composite wedges, Tuktoyaktuk coastlands, western arctic Canada. *Journal of Sedimentary Research* **66**: 17-25.
- Murton JB, Bateman MD. 2007. Syngenetic sand veins and anti-syngenetic sand wedges, Tuktoyaktuk coastlands, western arctic Canada. *Permafrost and Periglacial Processes* **18**: 37-47. DOI: 10.1002/ppp.577.
- Murton JB, French HM. 1993. Sand wedges and permafrost history, Crumbling Point, Pleistocene Mackenzie Delta, Canada. In: Proceedings of the Sixth International Conference on Permafrost, July 5-10, Beijing, China, South China Technological University Press, pp. 482-487.
- Murton JB, Worsley P, Gozdzik J. 2000. Sand veins and wedges in cold Aeolian environments. *Quaternary Science Reviews* **19**: 899-922.
- Péwé TL. 1959. Sand-wedge polygons (tessellations) in the McMurdo Sound region, Antarctica—a progress report. *American Journal of Science* **257**: 545-552.
- Sletten RS, Hallet B, Fletcher RC, 2003. Resurfacing time of terrestrial surfaces by the formation and maturation of polygonal patterned ground. *Journal of Geophysical Research* **108**, No. E4, 8044, doi:10.1029/2002JE001914.

Soil Survey Division Staff. 1993. *Soil Survey Manual*. Soil Conservation Service, U.S.

Department of Agriculture Handbook **18**.

Soil Survey Staff. 2006. *Keys to Soil Taxonomy (10th edition)*. United States Department of Agriculture, Natural Resources Conservation Service, Washington, D.C.

Sugden DE, Marchant DR., Potter N Jr, Souchez RA, Denton GH, Swisher CC,

Tison J-L. 1995. Preservation of Miocene glacier ice in East Antarctica. *Nature* **376**: 412
414.

Ugolini FC, Bockheim JG, Anderson DM. 1973: Soil development and patterned ground evolution in Beacon Valley, Antarctica. In: *Permafrost, North American Contribution to the Second International Conference*, 13-28 July, 1973, Yakutsk, U.S.S.R., National Academy of Sciences, Washington, D.C., 246-254.

Wang N, Zhao Q, Li J, Hu G, Cheng H. 2003. The sand wedges of the last ice age in the Hexi Corridor, China: paleoclimatic interpretation. *Geomorphology* **51**: 313-320.

List of Figures

Figure 1. Approximate position of outer Taylor II, III, IVa, and IVb moraines in lower and central Beacon Valley. Location of excavation sites for detailed examination of polygon centers and wedges is shown. Air photo by U.S. Geological Survey. The coordinates of sites 7-9 are 77°50'S, 161°00'E.

Figure 2. Photographs of an age-sequence of non-sorted sand-wedge polygons in Beacon Valley from a digital elevation model: (A) high-centered polygons with troughs 1-2 m wide on Taylor II drift in lower Beacon Valley (Black monitoring site 7); (B) a high-centered polygon with troughs 2-3 m wide on Taylor III drift in lower Beacon Valley (Taylor Glacier in the background is approximately 2 km away); (C) high-centered polygons with troughs up to 6 m wide on Taylor IV drift in central Beacon Valley looking southwest.

Figure 3. Selected areas of patterned ground from the Beacon Valley digital elevation model for three drift sheets on the valley floor showing the increasingly diffuse expression of high-center, sand-wedge polygons with time in Beacon Valley: (A) Regular pentagonal and hexagonal polygons on Taylor II drift in lower Beacon Valley (from oblique aerial photo); (B) poorly expressed polygons on Taylor III drift in lower Beacon Valley; and (C) diffuse polygons on Taylor IV drift in central Beacon Valley. The apparent fluting on Taylor III and IV surfaces may reflect prevailing wind ablation from the southwest to northeast or may represent aberrations in the DEM.

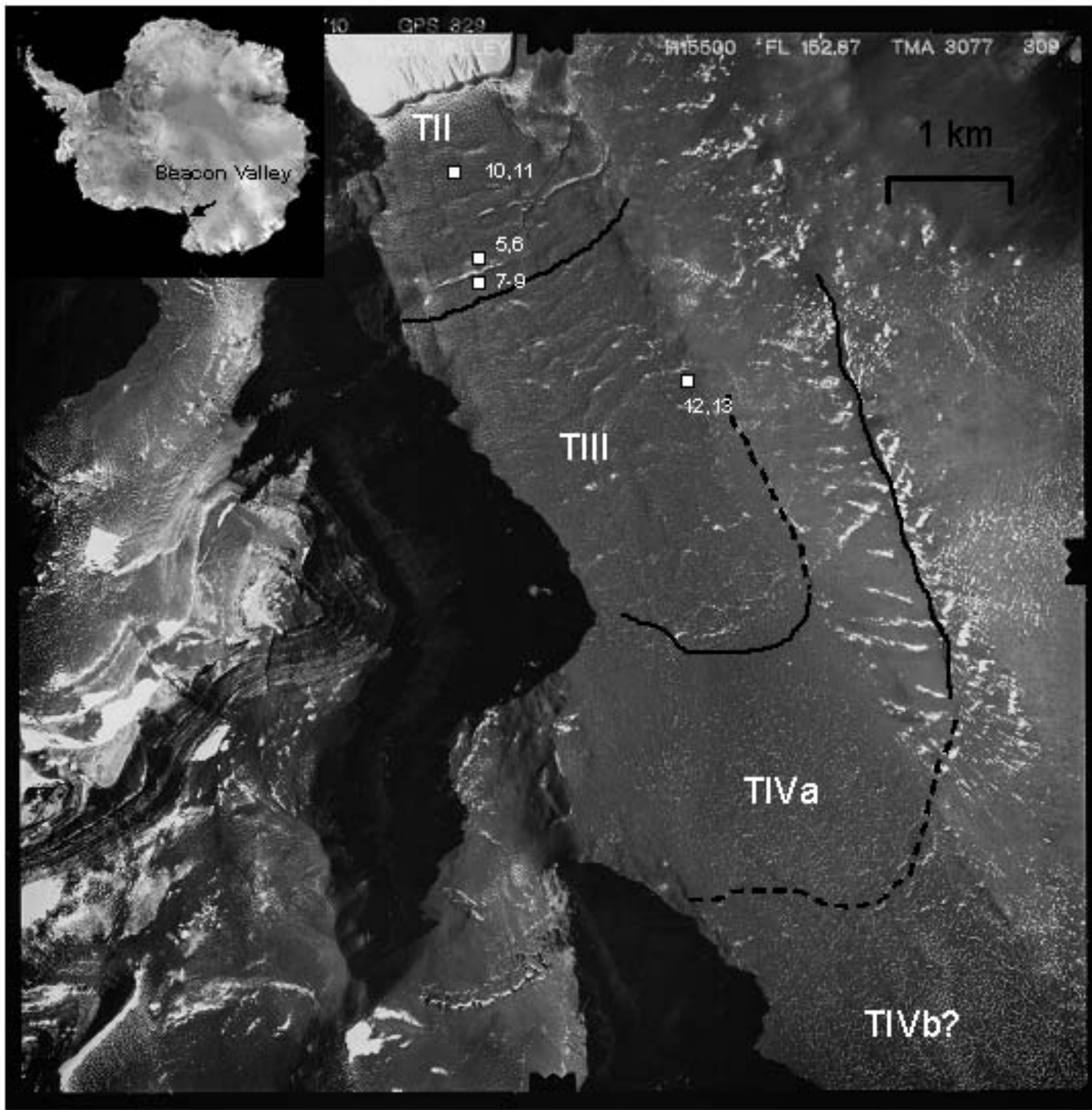
Figure 4. Selected photographs of sand-wedge excavations in Beacon Valley: (A) a wedge showing a fissure (arrow); (B) an exposed fissure (arrow) surrounded by ice-bonded permafrost; (C) and a series of inactive fissures (arrows) in a diffuse polygon (the fissures are spaced at approximately 10-cm intervals); (D) vertical laminations of sand as columns on stones (arrow) in

a sand wedge; (E) a lateral view of rivulets of flowing sand along a contraction crack; and (F) ice veins (arrow) in fissures of a sand wedge.

Figure 5. Cross sections of sand wedges on the innermost Taylor II moraine (A), the second-to-the-outermost Taylor II moraine (B), and on Taylor III drift (C).

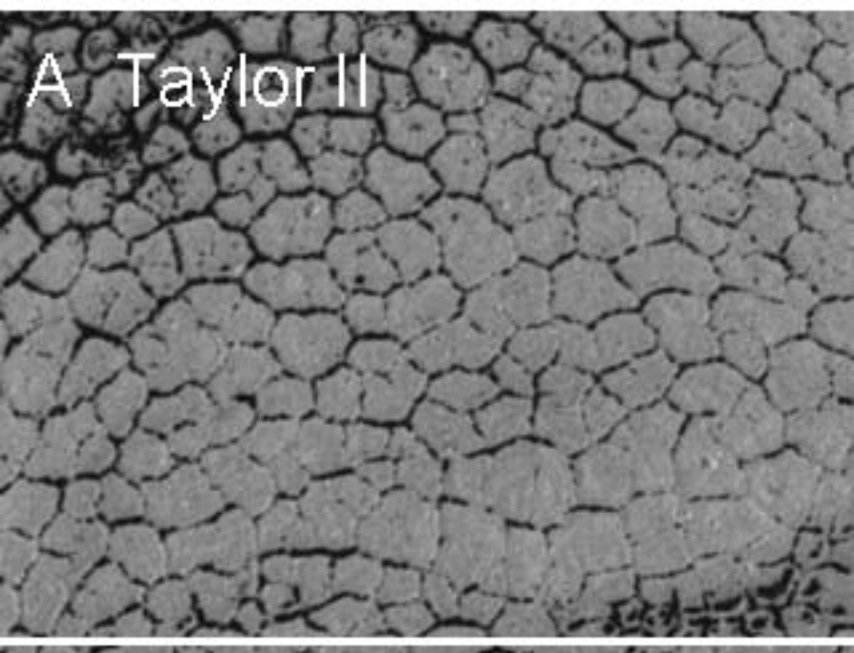
Figure 6. A model of sand-wedge polygon formation in lower and central Beacon Valley, Antarctica.

Figure 7. “Dimples” where sand is actively flowing down into a thermal-contraction fissure. The infilling sand originates from the side of the polygon and from aeolian addition. Note the lack of raised rims on the sides of the fissure.

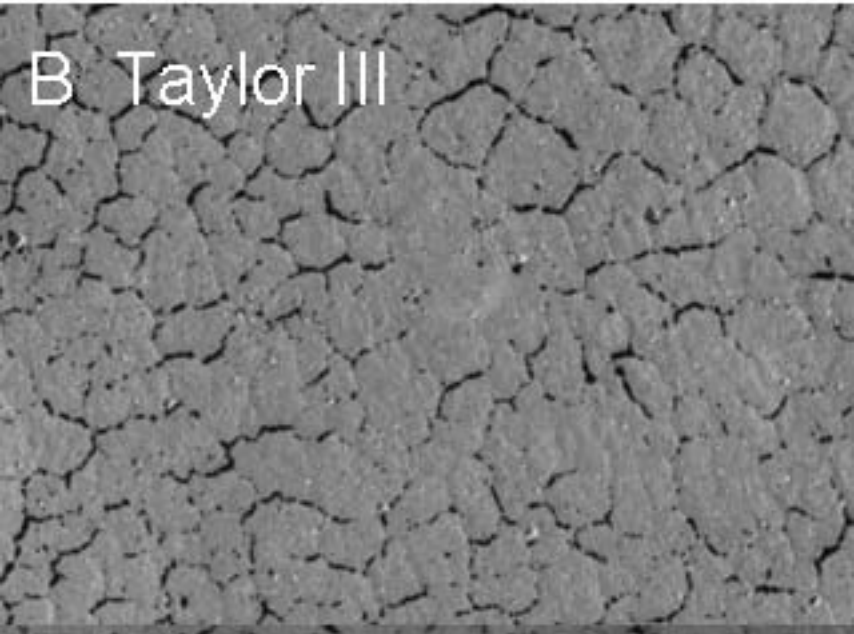




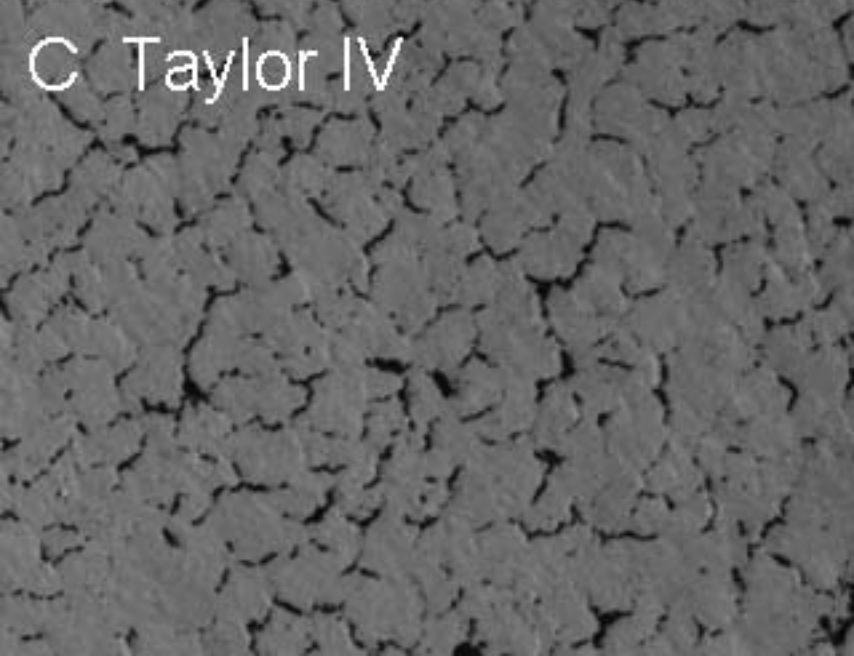
A Taylor II

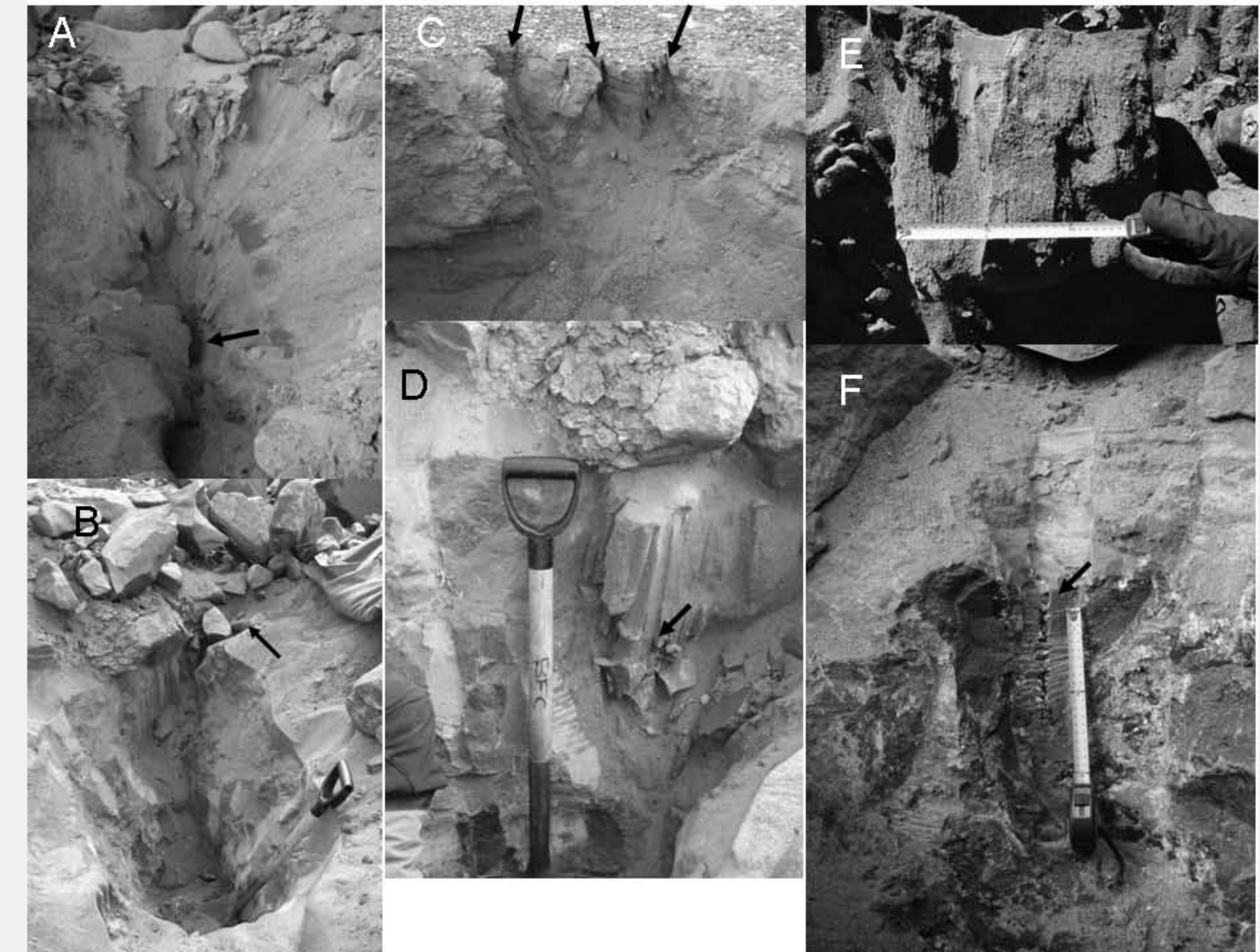


B Taylor III



C Taylor IV

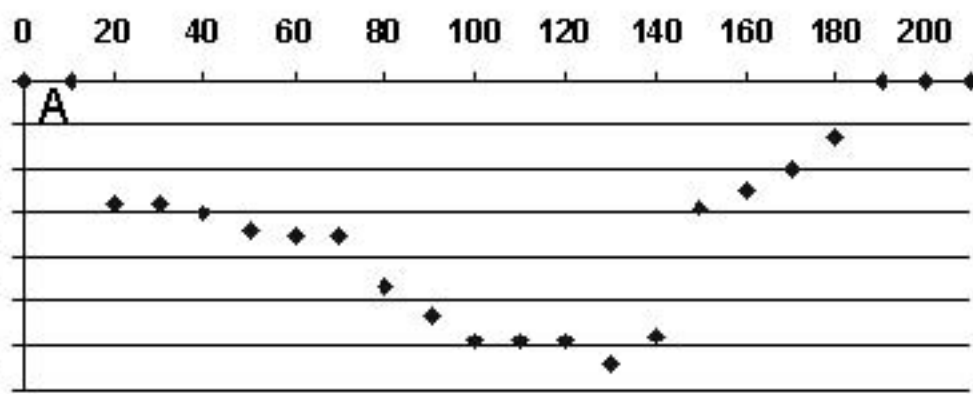




Distance across polygon fissure (cm)

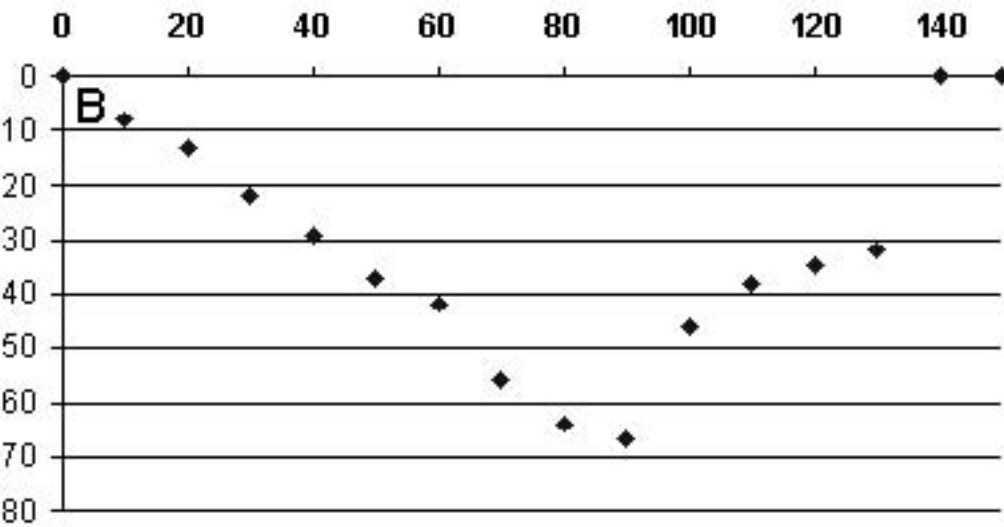
Polygon 4, Pit 8

Depth to ice-cemented permafrost (cm)



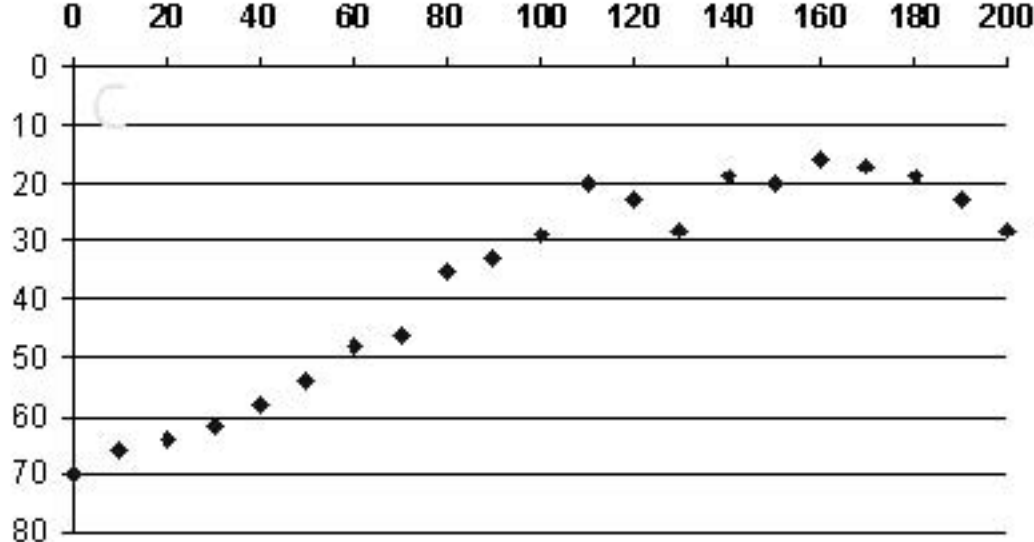
Polygon 5, pit 11

Depth to ice-cemented permafrost (cm)



Polygon 6, Pit 12

Depth to ice-cemented permafrost (cm)



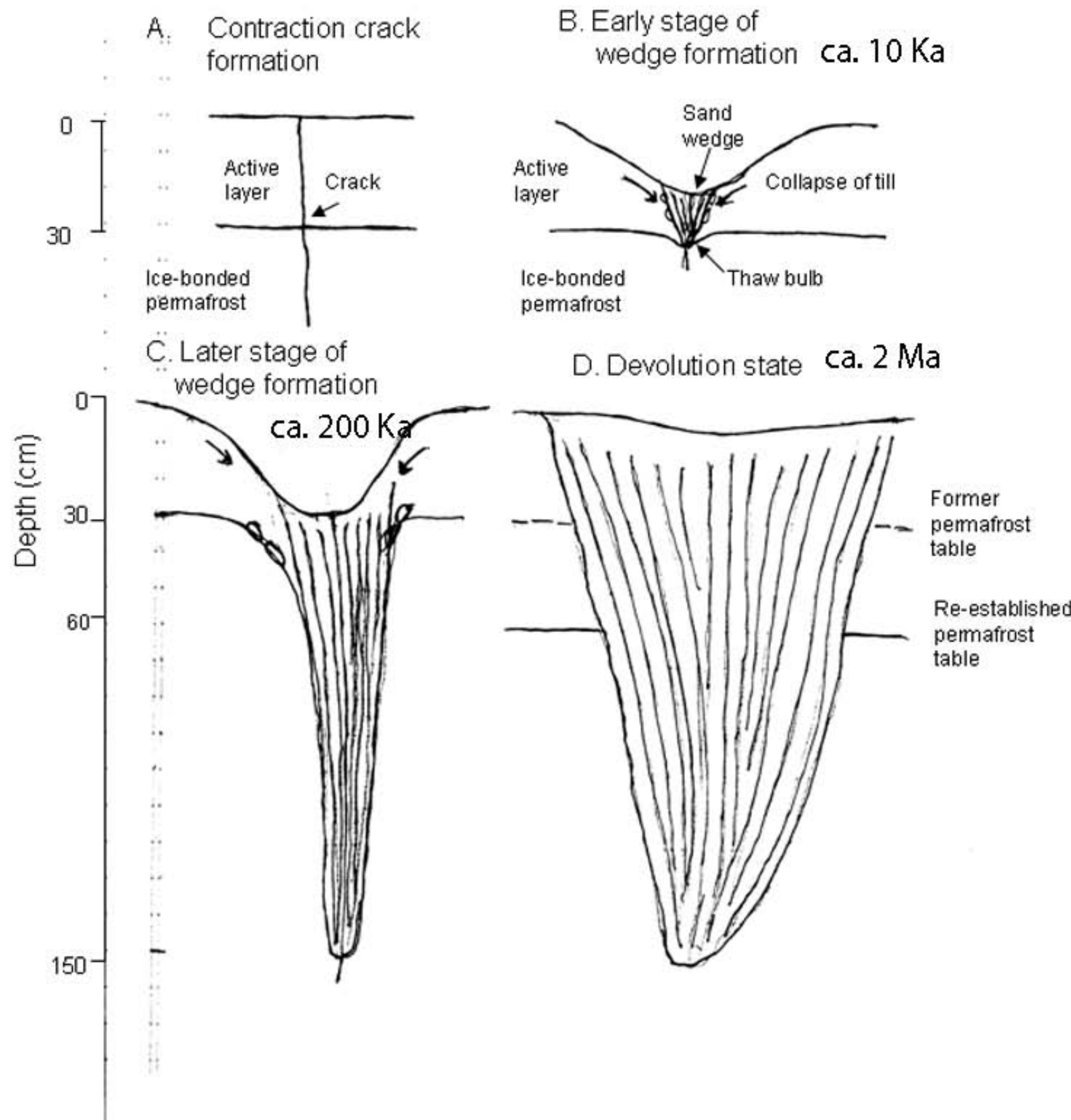




Table 1. Characteristics of sampling sites in Beacon Valley, Antarctica

Polygon No.	Pit No.	Polygon dimensions (m)	Polygon morphology	Wedge depth (m)	Wedge width. (m)	Location of pit	Geomorphic surface	Depth to ice bonding (cm)**	Total depth of excavation (cm)	Comments
3	5	10 x 11 (110 m ²)	high center			center	TIIc	12	50	ice-bonded permafrost contains rounded, frost qtz. xls, 48% interstitial ice; concrete-type frost
3	6			0.3-0.4	0.4-0.5	fissure		20/>90	90	ice lenses up to 5 mm thick and veins up to 1 cm wide; few gravels below 40 cm
4	7	10 x 8 (80 m ²)	high center			center	TIIc	26	75	buried ice at 39 cm; oblique sand-filled fissures in ice-bonded permafrost and vertical veins of sand and ice
4	8*			2.0	0.2-1.0	fissure		28/64	64	
4	9*			2.0	0.2-1.0	fissure		19/>86	86	no gravel; fissures filled with loose sand; concrete frost; vertical sand laminations 3 mm wide
5	10	10 x 11 (110 m ²)	high center			center	TII innermost	33	63	
5	11*			0.3-0.5		fissure		26/67	130	few gravel below 20 cm; vertical sand laminations as columns on clasts
6	12*	15.3 x 13.5 (207 m ²)	high center	1.5	2.0-2.5	fissure	TIII	16/70	90	secondary fissures; quartz grains rounded & frosted; fissures spaced at approximately 10-cm intervals across 2.5-m-wide primary wedge
6	13*			1.5	.15-2.0	fissure		45/79	110	buried ice at 92 cm; vertical fissures up to 45 cm deep; rounded quartz grains throughout; sand columns on clasts; few gravels
7	14	15 x 16 (240 m ²)	high center			center	TII outermost	62	100	ventifacts throughout; laminations in upper 20 cm
				0.5-1.5	0.3	fissure				

*Cross-sectional diagram prepared

**The slash shows minimum depth to ice bonding in the wedge and maximum depth beneath the thermal contraction fissure

Table 2. Morphometry of polygons in relation to drift sheet, Beacon Valley, Antarctica.

Drift sheet	Approximate age (yr) ¹	Polygon shape ²	No. of polygon sides visible	Polygon form ³	Mean polygon area (m ²)	Mean wedge width (m)	Mean wedge depth (m)
Taylor II	117 ka	R (4.5), P (38.6), H (27.3), S (27.3), O (2.3)	4-8	H (90), F (10)	100	0.5	1.0
Taylor III	200 ka	R (7.7), P (61.5), H (30.8)	4-6	H (80), F (20)	125	2.0	1.0
Taylor IVa	>1.0-<2.2 Ma	(not determined)	2-3	F (90), H (10)	125	3.0	0.5

¹ Brook et al., 1993; Sugden et al., 1995.

² Shape: R = rectangular; P = pentagonal; H = hexagonal; S = septagonal; O = octagonal (percentage of total given in parentheses).

³ Form: H = high-centered; F = flat-centered (percentage of total given in parentheses).

Table 3. Properties of soils in polygon centers and fissures of Beacon Valley.

Property	Polygon 7 Pit 14, Center	Polygon 5 Pit 10, Center	Polygon 5 Pit 11, Wedge	Polygon 3 Pit 5, Center	Polygon 3 Pit 6, Wedge	Polygon 4 Pit 7, Center	Polygon 4 Pit 8, Wedge	Polygon 4 Pit 9, Wedge	Polygon 6 Pit 12, Wedge	Polygon 6 Pit 13, Wedge	4 profiles Center ⁶	8 profiles Wedge ⁶
Geomorphic surface	TIIa	TIIb	TIIb	TIIc	TIIc	TIIc	TIIc	TIIc	TIII	TIII	TIVa	TIVa
Depth to base of oxidation (cm)	3-25	8.5	0	0	0	0	0	0	0-24	1-17	>34	>44
Maximum CDE ¹	24	24	12	12	12	12	12	12	30	24	22	23
Field texture ²	vks	ks	gs	gs	s	gs	gs	gs	gs	gs	ks	s
Depth to surface of ice-bonded permafrost	62	33	38-67	12	12-40	26	28-64	19-86+	16-70	45-79	>39	>43
Salt stage ³	2	1	1	1	0	1	0	0	1	1	1	1
Weathering stage ⁴	2	2	2	2	1	2	1	1	2.5	2.5	4	3.5
Depth of cohesive soil (cm)	62	9	67	12	0	0	0	0	24	7	>39	>44
Soil subgroup ⁵	THo	THo	THt	THo	THt	GHt	THt	THt	THt	GHt	TAo	THt

¹ Color Development Equivalents (Buntley and Westin, 1965)

² Texture: vks = very cobbly sand; ks = cobbley sand; gs = gravelly sand; s = sand.

³ Bockheim (1990)

⁴ Campbell and Claridge (1975).

⁵ THo = Typic Haplorthels; THt = Typic Hapluturbels; GHt = Glacic Hapluturbels; TAo = Typic Anhyorthels (Soil Survey Staff, 2006).

⁶ Bockheim (unpublished).

Table 4. Comparison of models explaining development of sand-wedge polygons in Beacon Valley, Antarctica.

Valley location	Parent materials	Mode of observation ¹	Deformation of adjacent strata ²	Change in height of polygon center	Evolutionary development	Number of development stages	Reference
entire	variable	sh ex	nd	lowered	retrogressive	2	Ugolini et al., 1973
upper	till/buried ice	sh ex	no	no change	retrogressive	4	Marchant et al., 2002
lower	till	sh ex, rd dis, cor	yes	raised	progressive	3	Sletten et al., 2003
upper	"debris"/buried ice	sh ex	nd	no change (deformed)	retrogressive	--	Levy et al., 2006
lower, central	till & till/buried ice	dp ex	no	lowered	retrogressive	3	this study

¹ Mode of development: sh ex = shallow excavation (<0.6 m); rd dis = rod displacement; cor = coring;
dp ex = deeper excavation (0.6-1.0 m)

² Nd = not determined.